Electronic Supplementary Material (ESI) for RSC Advances.

Supplementary Information

Effect of Nanoporous Structure and Polymer Brushes on the Ionic Conductivity of Poly(methacrylic acid)/Anode Aluminum Oxide Hybrid Membrane

Feng Chen[†a, b], Xiaoping Jiang[†a], Tairong Kuang[†b, c], Lingqian Chang[b], Dajiong Fu[b, c], Zhaogang Yang[b], Jintao Yang*[a], Ping Fan[a], Zhengdong Fei[a], Mingqiang Zhong*[a]

[a] College of Materials Science and Engineering, Zhejiang University of Technology, Hangzhou 310014, China.

[b] NSEC Center for Affordable Nanoengineering of Polymeric Biomedical Devices, The Ohio State University, Colombus, Ohio 43210, USA.

[c] National Engineering Research Center of Novel Equipment for Polymer Processing, South China University of Technology, Guangzhou 510640, China.

† These authors contributed equally to this work.

* Corresponding authors: Prof. Mingqiang Zhong, zhongmq@zjut.edu.cn; Dr. Jintao Yang, yangjt78@hotmail.com.

RAFT Polymerization of PMAA

The polymerization of MAA monomer was performed in ethanol The monomer concentration was kept constant at 16.7 wt%. The molar ratio of CPADB and ACVA were kept at 5:1. The polymerization of PMAA with 100 degree of polymerization is as follows. In a round-bottom flask equipped with magnetic stir bar 350 mg of CPADB (1.25 mmol) and 70 mg of ACVA (0.25 mmol) were dissolved in 2.15 mL of MAA (25 mmol). 13.6 mL of ethanol was finally added. After deoxygenation by nitrogen bubbling for 30 min, the resulting mixture was immersed in an oil bath thermostated at 70 °C. The reaction was stopped by inserting the flask in an ice bath and exposing the solution to air. The product was purified with dialysis against deionized water for 7 days. The regular withdrawal of samples allowed us to follow the evolution of monomer conversion. The monomer conversion was estimated by gravimetric analysis. Theoretical molar masses were obtained using the following equation:

$$Mn = \mathrm{M}_{\mathrm{monomer}} \times \frac{[\mathrm{monomer}]_0 \, x}{[\mathrm{CPADB}]_0} + \mathrm{M}_{\mathrm{CPADB}}$$

where M_n is the number-average molar mass, $M_{monomer}$ and M_{CPADB} are the molar masses of monomer and CPADB respectively, $[monomer]_0$ and $[CPADB]_0$ are the initial concentrations of monomer and CPADB respectively, and x is the fractional conversion of monomer .

Characterization of PMAA brushes

Gel permeation chromatography (GPC) was performed on a Waters-150C apparatus in DMF (0.05 m LiBr) at a flow rate of 1.0 mL/min using narrow molecular weight distribution poly (methyl methacrylate) as standards. ^{1}H NMR spectra were measured by using a Brucker ANANCE III 500 MHz NMR spectrometer with D_2O as a solvent.

As shown in Fig. S1, the polydispersity index (PDI) was 1.08, well below the theoretical lower limit of 1.50 for classical free-radical polymerization. Table S1 gives a summary of the molecular weights, PDI and percent conversions for the desired PMAA. The observed molecular weight as determined by GPC, corresponded very

closely to the theoretical molecular weights based on conversion, and indicated that the polymerization occurred in a controlled fashion.

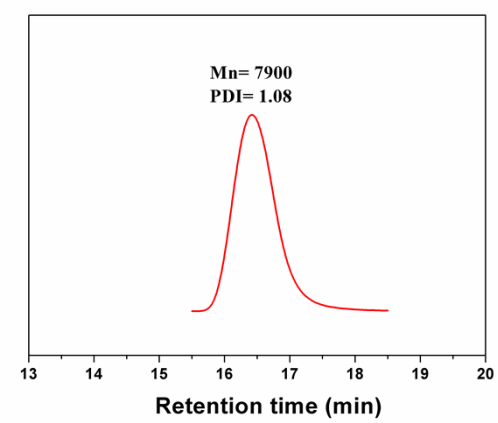

Fig. S1 The GPC curve of PMMA synthesized by RAFT polymerization.

Table S1 Summary of RAFT polymerization of PMAA.

DPn	M_n (Theory)	M_n (GPC)	PDI (M_w/M_n)	Conv. %
100	7600	7900	1.08	85

The purified PMAA was selected for ^{1}H NMR analysis. And the spectrum of refined sample affirmed the structures of the homo-polymer, indicating the successful polymerization. The result is shown in Fig. S2. The spectrum shows obtuse signals, which are caused by strong hydrogen bonds. It is clear that all the spectra show the signal of leaving groups of CPADB at lower field. This is an advantageous evidence of the successful RAFT polymerization of three kinds of electrolyte-type monomers.

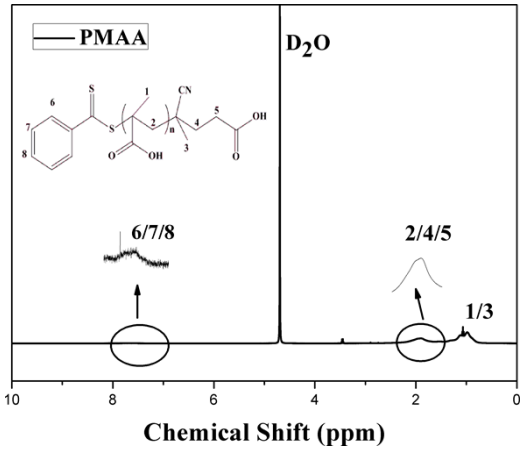

Fig. S2 The ^{1}H NMR spectrum of PMAA dissolved in D_2O solvent.

The radius of gyration (R_g) was measured by using static laser scattering (SLS) and dynamic laser scattering (DLS). The PAA sample was diluted to 1.0 mg/mL and maintained at 20 °C. A red laser (633 nm) was selected. Ten angles from 15° to 155° were performed during SLS test. The R_g was 2.0 nm measured by DLS. However, this is smaller than that of 7.3 nm measured by SLS. Fig. S3 presents the Zimm plots of PMAA sample.

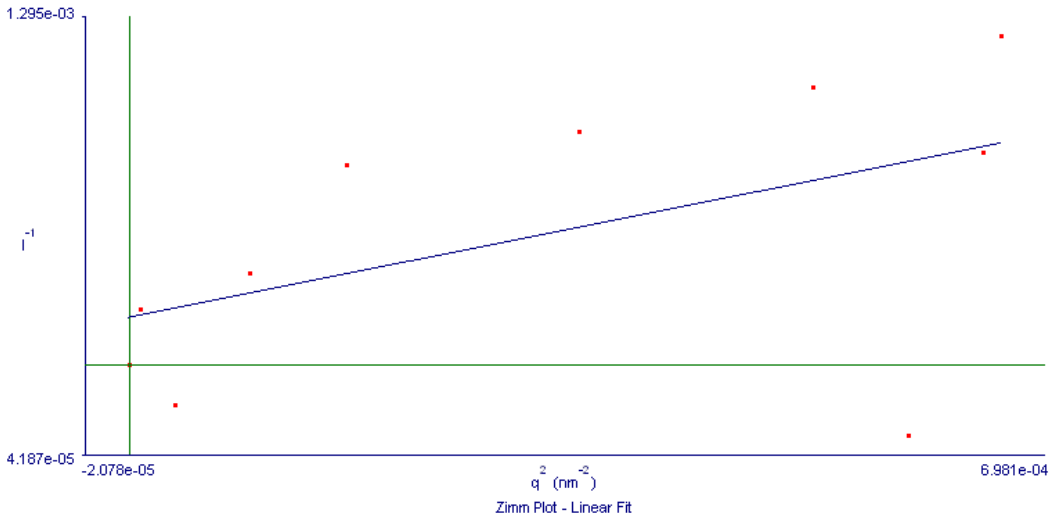

Fig. S3 Zimm plots of PMAA sample (1.0 mg/mL, 20 °C).

Characterization of AAO composite membranes

The "grafting-to" reaction mechanism is schematically shown in Fig. S4.

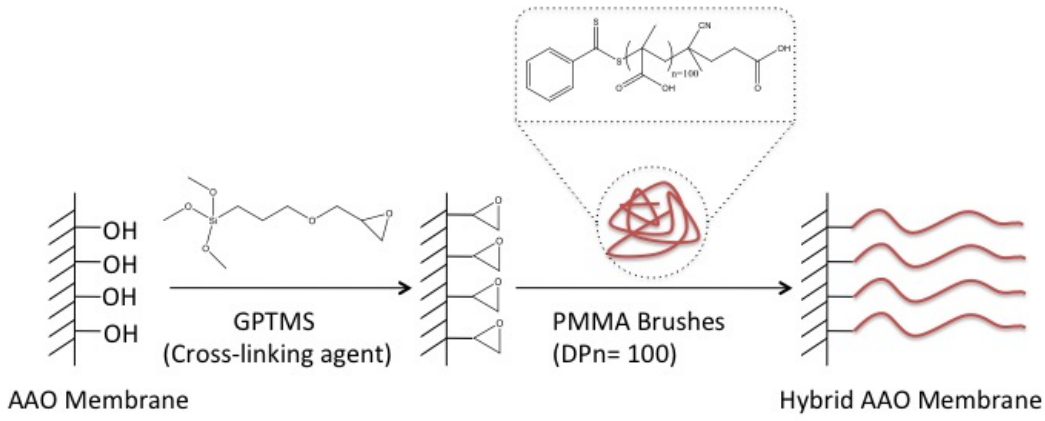

Fig. S4 The scheme of "grafting-to" mechanism.

The top surface of AAO membrane is observed by SEM analysis. And the represented SEM images are shown in Fig. S5. The AAO membranes consist of uniform and ordered nanopores.

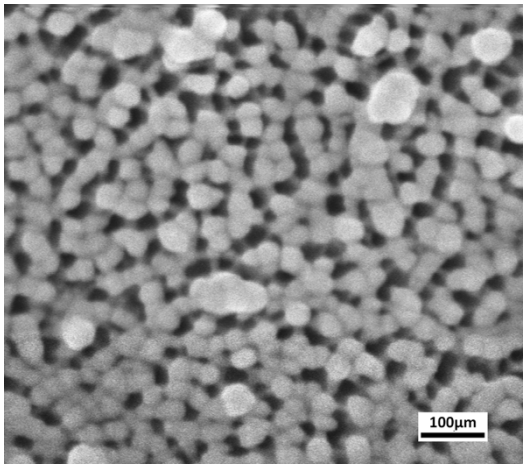

Fig. S5 The SEM images of top-view of 25 nm AAO membrane.

Since various nanopore sizes of AAO membrane and reaction conditions, SEM images depict different pore structures of AAO composite membranes. As a supplementary, Fig. S6 compare the modified nanopores with different grafting level. It is clearly shown that higher grafted amount of PMAA, narrower the modified pore size.

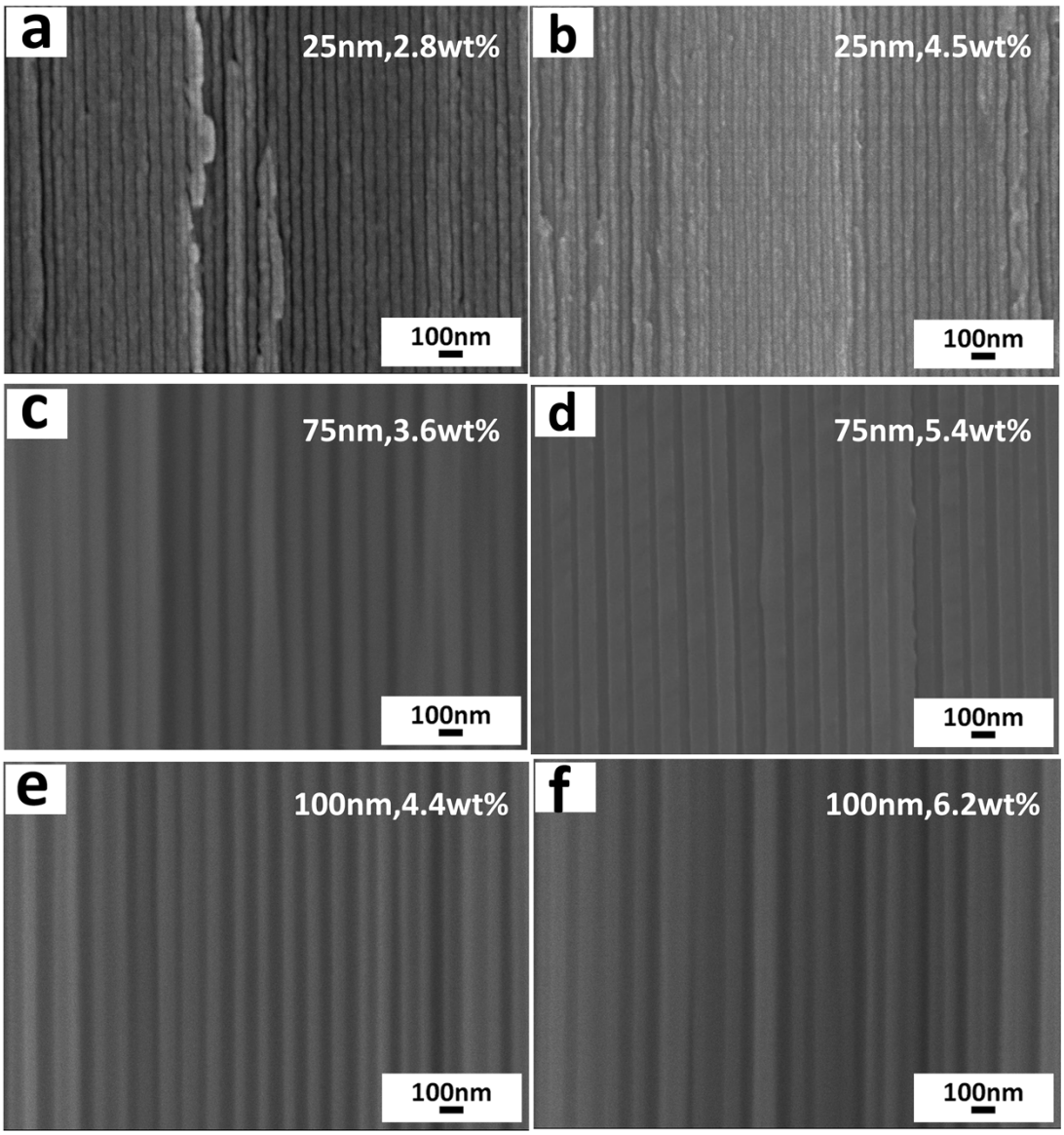

Fig. S6 SEM images of different pore structure of AAO composite membranes.

The endurance of hybrid AAO membrane

The pH value of solution is switched in turns and the ionic conductivity of hybrid membrane is recoded spontaneously. The results shown in Fig. S7 illustrate good endurance of hybrid AAO membrane.

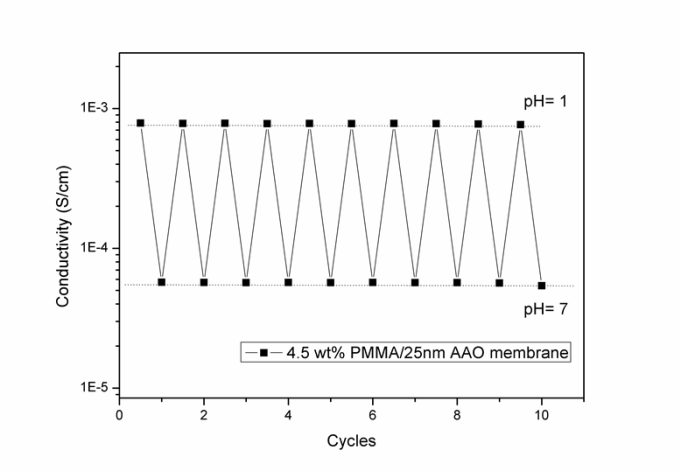

Fig. S7 The cycling switch of the ionic conductivity of hybrid AAO membrane.